Mol Biol Rep (2011) 38:1063–1070
DOI 10.1007/s11033-010-0203-2

PMS1 from *Arabidopsis thaliana*: optimization of protein overexpression in *Escherichia coli*

Celina Galles · Rodrigo L. Gomez · Claudia P. Spampinato

Received: 17 May 2010 / Accepted: 11 June 2010 / Published online: 23 June 2010

Abstract One of the major limitations when attempting to obtain detailed biochemical, biophysical and immunological characterization of plant DNA mismatch repair proteins is their extremely low abundance in vivo under normal growth conditions. An initial analysis of *PMS1* transcript level in various *Arabidopsis thaliana* tissues was carried out by quantitative real-time RT-PCR. For calli, flowers and seedlings, the corresponding cDNA copies per ng RNA were 66.9, 3.1 and 2.7, respectively. This suggests an important role of this gene in rapidly dividing tissues. In order to obtain a high level of PMS1 from *Arabidopsis thaliana*, the protein production was successfully optimized in an *Escherichia coli* host. The corresponding coding sequence of PMS1 was inserted into pET28a downstream a hexa-histidyl leader sequence. The pET28a–AtPMS1 plasmid was efficiently expressed in JM109(DE3)-pRIL strain probably due to the genotype features of the cells (*end*A1, *rec*A1, *rel*A1, *Δ(lac-pro*AB*)*, *laq*I*q*Z*Δ*M15) and the presence of extra copies of *argU*, *ileY*, and *leuW* tRNA genes, which encode the RIL codons. This strategy has allowed us to obtain His-tagged PMS1 at about 7% of the total soluble *E. coli* cell protein. The protein was purified by standard Ni^{+} affinity chromatography procedures and the electrophoretically homogeneous preparation was used as an antigen for antibody generation in rabbits. This approach provides effective tools for a further reconstitution of plant mismatch repair (MMR) system in vitro and for the analysis of protein expression and distribution of AtPMS1 in various tissues after different treatments (e.g. DNA mutagens).

C. Galles · R. L. Gomez · C. P. Spampinato (✉)
Centro de Estudios Fotosintéticos y Bioquímicos (CEFOBI), Facultad de Ciencias Bioquímicas y Farmacéuticas, Universidad Nacional de Rosario, Suipacha 531, 2000 Rosario, Argentina
e-mail: spampinato@cefobi-conicet.gov.ar

Keywords Mismatch repair · Real-time RT-PCR quantification · Heterologous expression · Polyclonal antibody

Introduction

The multiple eukaryotic homologs of the bacterial MutL mismatch repair protein are implicated along with MutS homologs in maintaining genomic integrity during DNA replication and recombination (reviewed in [1–5]). Four MutL homologues encoded by yeast and mammals form three functionally different heterodimers. MutLα, the heterocomplex of MLH1–PMS1 in yeast and MLH1–PMS2 in humans, represents the major MutL activity involved in the post-replicative repair [6–9], where it coordinates the mismatch recognition step by MutS homologs to downstream events that finally lead to the substitution of the error-containing strand with an accurate copy of the template sequence. Mutations in MLH1 or PMS2 result in a mutator phenotype which has been directly linked to increased susceptibility to hereditary nonpolyposis colon cancer (HNPCC) in humans (reviewed in [10]).

All members of MutL family contain a set of conserved aminoacid motifs near the amino terminal end that are common to the GHKL protein family and form a nucleotide binding pocket [11–14]. ATP binding and very weak ATPase activity were demonstrated for *Escherichia coli* MutL [15], human PMS2 [16] and *Saccharomyces cerevisae* MLH1 and PMS1 [17]. These ATPase activities are required for normal mismatch repair function [17, 18]. In addition to binding and hydrolyzing ATP, MutL homologues bind single- and double-stranded DNA in a sequence and mismatch independent manner [15, 19–21]. In addition to ATP

and DNA binding, eukaryotic MutL proteins have an endonuclease motif on the PMS1(PMS2) subunit that incises the discontinuous strand and thus generates new entry sites for the 5′–3′ exonuclease EXOI to remove the mismatch [22–24]. In *Arabidopsis thaliana*, three MutL homologs designated as MLH1, PMS1 and MLH3 have been identified [25–27]. MLH1–MLH3 heterodimer appears to play an important role in promoting meiotic crossovers [27], while the MLH1–PMS1 heterodimer (AtMutLα) is proposed to function in the correction of different classes of DNA mismatches according to yeast and mammal homologues. A more detailed biochemical and structural characterization requires high level production of the protein complex.

In this work, we evaluate the expression of the At*PMS1* gene (At4g02460) in calli, flowers and seedlings by quantitative real-time PCR. We then report the first PMS1 protein over-expression in *E. coli* and its purification to homogeneity. We have also raised polyclonal-antibodies against the PMS1 subunit. The described approaches can be useful for a further biochemical and structural characterization of this *A. thaliana* protein and for the in vivo study of protein expression in response to endogenous and exogenous DNA mutagens.

Materials and methods

Chemicals and reagents

Trizol reagent and Zero Blunt TOPO PCR Cloning Kit were purchased from Invitrogen. M-MLV reverse transcriptase and β-isopropyl-D-thiogalactoside (IPTG) were from Promega. Restriction enzymes were products from New England Biolabs or Promega. Monoclonal anti-His antibody and HisTrap HP columns were from Amersham Biosciences. Anti-mice and anti-rabbit IgG antibodies conjugated to alkaline phosphatase were obtained from Bio-Rad. All other chemicals and reagents used were of molecular biology grade.

Plant material and growth conditions

Arabidopsis thaliana (Columbia ecotype) plants were grown at 25°C in a growth room with a 16 h photoperiod. Leaves from 3-week-old plants were either immediately processed or quickly frozen in liquid nitrogen and stored at −80°C until use. Callus formation was induced by incubation of surface sterilized seeds on Murashige and Skoog basal salt (MS) [28] medium supplemented with 3% (w/v) sucrose, 0.5 mg/l kinetine, 2.5 mg/l 2,4-dichlorophenoxyacetic acid and 2.5% (w/v) phytagel for 72 h at 4°C. Calli were cultivated on the same medium under dark conditions at 22°C.

Bacterial strains and growth conditions

Escherichia coli strains DH5α, BL21-CodonPlus (DE3)-pRIL (Stratagene), BL21(DE3)-pLysS (Novagen) and JM109(DE3) carrying the pRIL (Stratagene) or the pLysS (Novagen) plasmids were used in cloning or expression experiments. Cells were grown in LB medium in the presence of kanamycin (30 μg/ml), nalidixic acid (15 μg/ml) and/or chloramphenicol (20 μg/ml) where appropriate. Agar (1% w/v) was added to solid media.

Analysis of AtPMS1 transcript by quantitative real time PCR

Total RNA was isolated from about 100 mg of various *A. thaliana* tissues using the TRIzol reagent (Invitrogen) as described by the Manufacture's Protocol. All RNA samples were incubated with RNase-free DNase I (1 U/ml) to remove traces of genomic DNA. Reverse transcription was performed with 4 μg of RNA using SuperScript II reverse transcriptase (Invitrogen) and oligo-dT as a primer in a final volume of 20 μl. After reverse transcription, 1 μl of a 1:3 dilution of the cDNA obtained was used as template for real time PCR with a Mx 3000P QPCR System (Stratagene, La Jolla, CA) using a reaction mixture containing 332.5 nM forward (CTCCTGGAACACAAGCTGAT) and reverse (TTTAGGACCGGTTGACTG) specific primers spanning a 200-bp region of At*PMS1* cDNA, 20 mM Tris–HCl, pH 8.5, 50 mM KCl, 0.5x SYBR Green I (Invitrogen), 3.5 mM $MgCl_2$, 0.23 mM dNTPs and 0.58 U Platinum Taq DNA polymerase in a total volume of 20 μl. The PCR thermal cycling conditions were 2 min denaturation at 94°C, followed by 50 cycles of 96°C denaturing for 10 s, 57°C annealing for 15 s, and 72°C extension for 20 s and a final extension step at 72°C for 1 min. After each real time reaction, the amplification products were verified by 2% (w/v) agarose gel electrophoresis and melting curves were analyzed to ensure the identity of the specific PCR product. The absolute copy number of At*PMS1* mRNA was calculated with standard curves performed with serial dilutions of the pET28a–AtPMS1 plasmid as template DNA. Based on the molecular weight of the cloned DNA, the concentration of the template applied in each reaction ranged from 0.25 fg to 0.25 ng. All reactions were performed in triplicate from two independent sets of biological replicates and each real time PCR experiment was conducted at least twice.

Cloning of *A. thaliana* PMS1 homolog

Total RNA was isolated from young leaves of *A. thaliana* using Trizol reagent as described by the manufacturer. The first-strand cDNA was synthesized by M-MLV reverse

transcriptase using total RNA as the template and oligo(dT)$_{16}$ as the primer. The PMS1 coding region (GenBank Accession No. AY047228) was PCR amplified using the forward primer AtP1-5PVsp: 5′-GTCATTAATACCA TGCAAGGAGATTCTTCTCCG-3′ containing an artificial *Vsp*I site and the reverse primer AtP1-3PBam: 5′-CTGG GATCCTCATGCCAATGAGATGGTTGC-3′ containing a unique *Bam*HI site. PCR reaction was carried out by a denaturation step at 96°C for 5 min, followed by 40 cycles (30 s at 94°C, 30 s at 60°C and 3 min at 72°C), and a final extension at 72°C for 7 min in a Gene Amp PCR System 2400 (Perkin-Elmer). The proofreading Vent DNA polymerase was used to synthesize the PCR fragment. The product was subcloned into the pCR-Blunt II-TOPO vector yielding the intermediate construction named pTOPO–AtPMS1. Positive clones were transformed in *E. coli* DH5α and plasmids were prepared using QIAprep kit. pTOPO–AtPMS1 was digested with *Vsp*I/*Bam*HI and the product was loaded on agarose gels. The correct band was excised and purified using QIAquick Gel Extraction kit. The resulting *Vsp*I/*Bam*HI fragment containing the entire PMS1 coding region was ligated into the *Nde*I/*Bam*HI sites of pET28a (Novagen) in frame with the His$_6$-tag to yield the final pCG01 plasmid.

Cell growth

Recombinant pCG01 plasmid containing *pms1* cDNA from *A. thaliana* was transformed in four different electrocompetent *E. coli* host cells: BL21-CodonPlus (DE3)-pRIL, BL21-CodonPlus (DE3)-pLysS, JM109(DE3)-pRIL and JM109(DE3)-pLysS following standard electroporation procedures [29]. An isolated fresh transformant was inoculated into 5 ml LB medium containing the antibiotics according to the particular plasmids (30 μg/ml kanamycin, 15 μg/ml nalidixic acid and/or 20 μg/ml chloramphenicol). This culture was incubated overnight at 37°C with vigorous shaking. Afterwards, the necessary inoculums that would provide an initial $OD_{600nm} \approx 0.05$ were inoculated into 200 ml LB medium containing antibiotics followed by incubation at 30°C up to an OD_{600nm} of 0.8–1.0. At this point AtPMS1 expression was induced by the addition of IPTG to a final concentration of 0.1 mM. Aliquots were collected immediately for the uninduced control or after additional cell growth for 3, 6, and 16 h at 16°C.

Stability and toxicity of PMS1 expression vector

Serial dilutions (from 10^{-2} to 10^{-8}) were prepared for uninduced and induced cultures grown as indicated above. Five μl of each dilution were plated on LB-agar plates in the presence or absence of kanamycin to check plasmid stability. At the same time, the toxic effects of AtPMS1 protein expression were tested on LB-kanamycin-agar plates containing 0.5 mM IPTG. The stability and toxicity of the plasmids were determined by estimating the number of colony-forming units of each dilution on the respective plates. Absence of colonies on plates containing kanamycin or both kanamycin and IPTG as compared to control plates (plain LB-agar plates or LB-kanamycin) were interpreted as plasmid loss and toxicity, respectively.

Recombinant expression and purification of AtPMS1

Overnight induced cultures were harvested by centrifugation at 5,000*g* for 20 min at 4°C. The cell pellets were then immediately either stored at −80°C or resuspended in 15 ml/g cell wet weight chilled binding buffer (20 mM Tris–HCl, 30 mM imidazole, 0.5 M NaCl, pH 7.4, 1 mM PMSF). Alternatively, the induced AtPMS1 cell pellet was resuspended in lysis buffer containing 20 mM potassium phosphate, pH 7.4, 5 mM KCl, 1 mM $MgCl_2$, 1 mM PMSF. When indicated cells were sonicated for 2 min in 10 s pulses with 30 s between pulses in an ice bath and the cell debris was then removed by centrifugation at 7,000*g* for 20 min at 4°C. Uninduced and induced cultures, both soluble and insoluble fractions, were analyzed by 8% (w/v) SDS-PAGE and proteins were detected with Coomassie Brilliant Blue stain. In addition, JM109(DE3)-pRIL strains were transformed with the expression vectors lacking the insert and used as controls.

AtPMS1 protein purification was carried out with the resulting soluble cell extracts. The supernatant was filtered through a 0.2 μm cellulose acetate membrane and loaded onto a HisTrap HP affinity column previously equilibrated with binding buffer. The column was exhaustively washed with the same buffer to remove unspecific proteins bound to the resin. Finally, increasing imidazole concentration to 500 mM in the same buffer allowed elution of the attached AtPMS1 protein. Aliquots of the various fractions were analyzed by SDS-PAGE and subsequent staining or electroblotting (see below).

Antibody generation

Standard procedures were used to raise polyclonal-antibodies against AtPMS1 protein in rabbits. A sample of purified denatured recombinant protein (200 μg) was mixed with Freund′s complete adjuvant (1:1 ratio) and then injected subcutaneously into a 4-month-old white rabbit. A boost of the same protein (100 μg) was injected at 3-week intervals. After 25–28 days of the last injection, antiserum was collected and subsequently AtPMS1 antibodies were purified according to a procedure described previously [30]. Briefly, recombinant AtPMS1 protein was subjected to SDS-PAGE (8% w/v) and Western blotting. AtPMS1 was

detected by reversibly staining with Ponceau S and excised from the nitrocellulose membrane. The membrane slice was then blocked for 1 h at 4°C with 5% (w/v) skim milk powder in TBS buffer containing 10 mM Tris–HCl buffer, pH 7.5, and 150 mM NaCl. Following three 5 min-washes with TBS buffer, the slice was incubated with 0.5 ml of antiserum for 1 h at 4°C. After another three 5 min-washes with TBS buffer, addition of 500 µl of 100 mM glycine–HCl, pH 3.0 and 100 mM NaCl allowed elution of the bound antibodies. Finally, the pH of the solution was adjusted to pH 7.5 by the addition of 1 M Tris–HCl, pH 8.0. The antibody elution step was repeated 3 times and the whole affinity-purification protocol was performed four-times in all. All the fractions containing the antibodies were pooled, brought to 0.02% (w/v) NaN_3, and stored at −80°C.

SDS-PAGE and immunological analyses

Protein samples were analyzed on 8% (w/v) polyacrylamide/bisacrylamide denaturing gels according to Laemmli [31]. After electrophoresis with the Bio-Rad Mini-Protean 3 system at 40 mA, proteins were either visualized by staining with Coomassie brilliant blue (R250) [31] or electroblotted on nitrocellulose membranes (Bio-Rad) at 50 V for 1 h [32]. After protein transfer, the membrane was stained with Ponceau S to check transfer efficiency and then blocked with 5% (w/v) skim milk powder in TBS buffer to minimize unspecific protein/antibodies binding. All further steps were carried out in TBS buffer. Immunodetection of the His-tagged fusion protein was carried out with commercially available anti-His antibodies (1:3,000 dilution) followed by incubation with rabbit anti-mice IgG conjugated to alkaline phosphatase. Alternatively, AtPMS1 was immunodetected with the affinity purified anti-AtPMS1 (2 µg/ml) polyclonal antibodies described above and recognized by goat anti-rabbit IgG conjugated to alkaline phosphatase. Afterward, membranes were developed with 5-bromo-4-chloro-3-indolyl phosphate and nitro blue tetrazolium [32].

Analytical methods

Protein concentration was quantified using Bradford reagent (Bio-Rad) and BSA as the protein standard [33]. Cell growth in liquid media was determined by measuring the absorbance at 600 nm using a UNICAM, HEλI0S β spectrophotometer.

Results and discussion

At present, plant DNA MMR system is by far much less characterized than the respective prokaryotic, yeast and mammalian mechanisms. So far, studies performed in plants are restricted to the identification of MutS and MutL homologs and analysis of T-DNA insertion mutants. Furthermore, MutL homologs have been characterized in plants to a more limited extent than MutS homologs. *MLH1* and *PMS1* genes from *A. thaliana* have been identified [25, 26] and the roles of the corresponding proteins have been studied by gene inactivation (see [34] for a recent review). Disruption of *MLH1* and *PMS1* generated an accumulation of frameshift mutations and an increase in the frequency of homeologous recombination [35–38]. Additional biochemical and biophysical data of the individual plant mismatch repair proteins is still lacking probably due to their low abundance in vivo and the lack of an efficient and large-scale heterologous host protein production system. Here, we first analyzed the *PSM1* gene expression by quantitative real time RT–PCR in calli, flowers and seedlings from *A. thaliana*. Then, we constructed a prokaryotic system to overexpress the protein in *E. coli*. As far as we know, this is the first successful AtPMS1 overexpression in *E. coli*. The results obtained may allow future investigation on the biochemical, structural and immunological characterization of PMS1 and the in vitro mechanism of action of plant DNA mismatch repair system.

Analysis of AtPMS1 mRNA expression

At*PMS1* transcript level was evaluated by quantitative real time RT-PCR. Previous reports indicate that this gene shows higher expression in cultured cells than in seedlings when analyzed by Northern blot [25]. Here, the starting copy number of the At*PMS1* gene was quantified in calli, flowers and seedlings using standard curves generated with the pET28a-PMS1 plasmid. Based on the known molecular weight of the cDNA, the amount of template applied in each reaction ranged from 0.25 ng to 0.25 fg. As shown in Fig. 1, the expression of *PMS1* per ng total RNA increased in the order calli > flowers ≥ seedlings (66.9, 3.1 and 2.7 cDNA copies/ng RNA, respectively). These data confirm that *PMS1* gene is strongly required to ensure genomic stability in rapidly dividing tissues. Further analysis using Genevestigator indicate that *PMS1* is more strongly transcribed in calli than in the other two tissues (Fig. 1, inset), thus validating our real time PCR data.

AtPMS1 expression constructs

At*PMS1* cDNAs was obtained by RT-PCR using specific primers. After amplification, the cDNA encoding At*PMS1* was inserted into the pET28a expression vector so that the *pms1* sequence is in frame with an *N*-terminal His_6-tag leader sequence. This His_6-tag fusion facilitates the purification of recombinant protein by Ni^{2+} affinity chromatography and immunodetection by anti-His-tag antibodies.

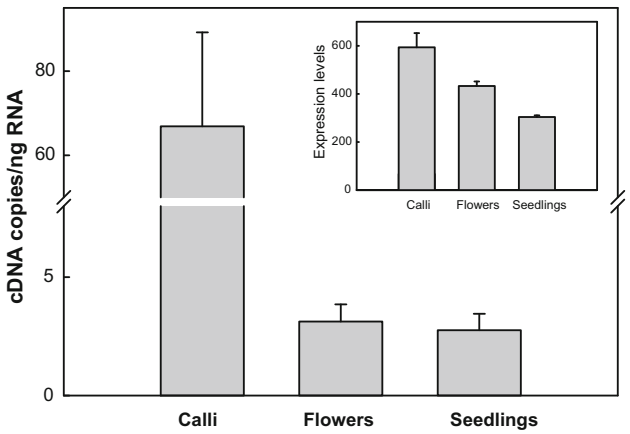

Fig. 1 Expression profiles of At*PMS1* gene. Absolute copy numbers of At*PMS1* transcript in calli, flowers and seedlings were calculated by quantitative real time RT-PCR using standard curves performed with serial dilutions of the pET28a–AtPMS1 plasmid as template DNA. Based on the molecular weight of the cloned DNA, the concentration of the template applied in each reaction ranged from 0.25 fg to 0.25 ng. *Inset*: At*PMS1* expression analysis performed using the Genevestigator database

AtPMS1 toxicity and expression assay

Plasmid instability and toxicity mediated by IPTG induction of AtPMS1 expression were compared in four *E. coli* strains: BL21-CodonPlus (DE3)-pRIL, BL21(DE3)-pLysS, JM109(DE3)-pLysS and JM109(DE3)-pRIL. As indicated, plasmid loss and toxicity were analyzed by comparing plating efficiency on antibiotic or both antibiotic and inducer to that on plain or antibiotic plates, respectively. As shown in Fig. 2, plasmid pCG01 was stable in all assayed strains (compare columns in the absence of any addition and in the presence of selection marker). However, when serial dilutions of the assayed strains induced with IPTG were plated on LB-agar medium containing IPTG, there was a significant inhibitory effect on colony-forming units only for JM109(DE3)-pRIL and BL21-CodonPlus (DE3)-pRIL strains (shown on the right column of Fig. 2). On the other hand, viable colonies were observed for BL21(DE3)-pLysS and JM109(DE3)-pLysS in the presence of IPTG. This result rules out the possibility of IPTG as responsible for the observed toxicity in bacteria carrying the RIL plasmid.

Subsequently, all the cultures were examined for their ability to express PMS1. No overexpression of the protein was observed in cell cultures of strains harboring the pLysS plasmid as shown by an SDS-PAGE stained with Coomassie Brilliant blue (Fig. 3a). In contrast, the target protein was well overexpressed in JM109(DE3)-pRIL after 16 h induction with 0.1 mM IPTG (Fig. 3a). The protein was also induced in BL21-CodonPlus (DE3)-pRIL under the same conditions (Fig. 3b). Thus, the presence of *argU*, *ileY* and *leuW* tRNA genes in the RIL plasmid was an important contributing factor for increasing translation efficiency. In fact, *A. thaliana PMS1* gene uses these rare tRNAs (5.8%) whereas these are less represented in MutL *E. coli* (1.8%). The strategy of increasing rare tRNA genes within the host has been employed at several laboratories to improve heterologous expression yields [39].

The results described indicate a relation between protein overproduction and the inhibition of colony formation. The target protein was expressed in BL21-CodonPlus (DE3)-pRIL and JM109(DE3)-pRIL despite a considerable lack of colony-forming units mediated by IPTG, suggesting that PMS1 induction is linked with colony growth. Even more, colony formation of JM109(DE3)-pRIL cells after 16 hs induction of the recombinant protein with 0.1 mM IPTG

Strain	Construction	Time after induction (hs)	Addition		
			None	Selection marker	Selection marker and IPTG
BL21(DE3)pLysS	pCG01	0			
		16			
BL21-CodonPlus (DE3)-RIL	pCG01	0			
		16			
JM109(DE3)-pLysS	pCG01	0			
		3			
		6			
		16			
JM109(DE3)-pRIL	pCG01	0			
		3			
		16			

Fig. 2 Comparison of plasmid stability and toxicity mediated by heterologous protein expression in various *E. coli* hosts. Kanamycin (30 μg/ml), chloramphenicol (20 μg/ml) and/or IPTG (0.5 mM) were added to LB-agar plates where appropriate. Each spot of each panel from left to right corresponds to culture dilutions from 10^{-2} to 10^{-8}. Toxicity induced by protein expression is defined as the absence of colonies on LB-antibiotics-IPTG agar plates

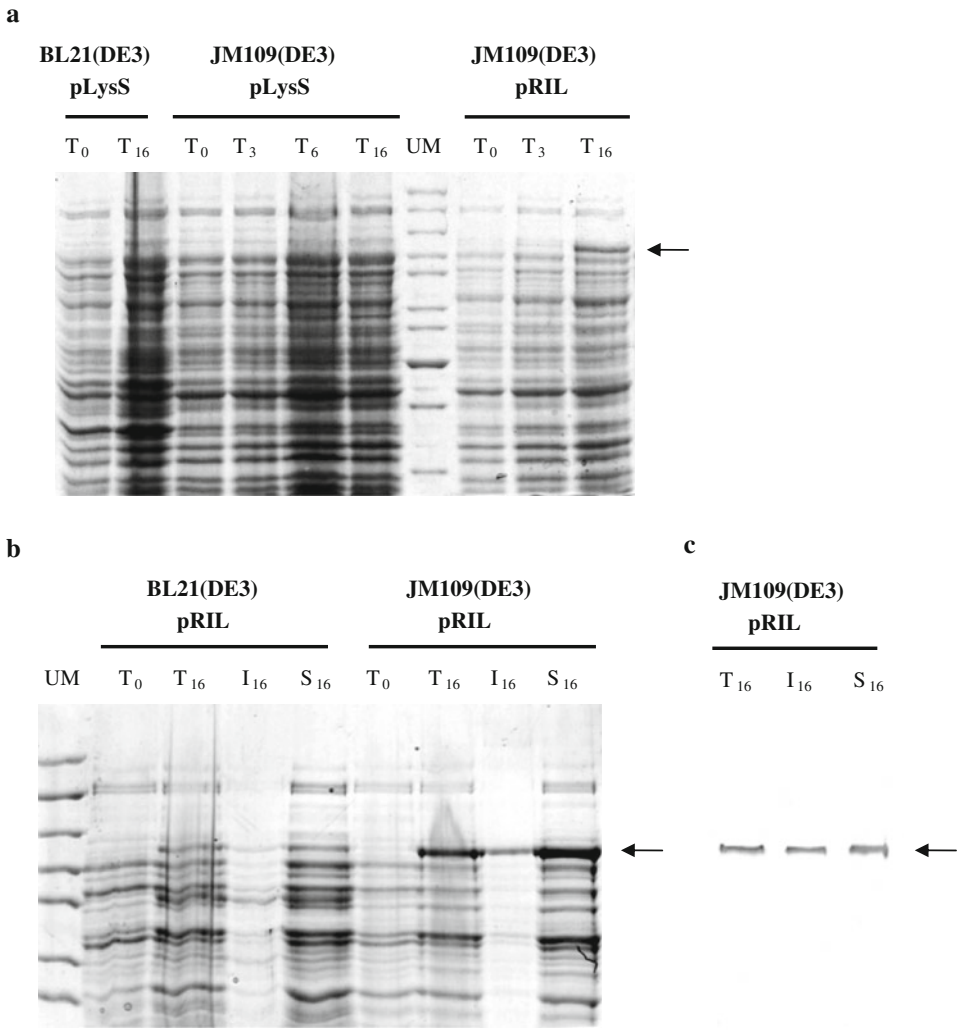

Fig. 3 Expression analysis of AtPMS1-pET28a in various *E. coli* strains. Cell extracts were electrophoresed on SDS-PAGE gels and proteins were visualized by Coomassie blue staining (**a**, **b**) or Western-blot (**c**). Strains used are indicated above the respective lanes. *Lanes* T_0, T_3, T_6, T_{16}: total fractions before and after 3, 6 and 16 h induction with IPTG. Lanes S_{16} and I_{16}: soluble and insoluble fractions recovered after sonication of the overnight induced cultures, respectively. Lane UM: unstained molecular mass markers whose values from top to bottom were 200, 150, 120, 100, 85, 70, 60, 50, 40 kDa. The *arrow* indicates the position of the overexpressed fusion protein at the expected position

was inhibited (Fig. 2, last row), confirming that the overexpression of PMS1 was toxic to *E. coli*.

AtPMS1 expression and purification

Freshly single transformants were grown in liquid LB media and induced by IPTG. Cells were harvested and disrupted under the indicated conditions. The cell lysate was clarified by centrifugation and both soluble and insoluble fractions were analyzed on SDS-PAGE. As shown on Fig. 3b, AtPMS1 expression yield in JM109(DE3)-pRIL was much higher than that in BL21-CodonPlus (DE3)-pRIL. Expression efficiency in JM109(DE3)-pRIL cells might have improved significantly due to the presence of an extra source of *lacI*^{q} repressor protein, complete *lac* deletion and *endA, relA* and *recA* mutations in JM109(DE3) cells, which might be responsible for tightly controlling basal expression and improving plasmid quality and stability. Although yeast and human PMS1 were reported to be unstable in the absence of their counterpart MLH1 [40, 41], we successfully overproduced PMS1 individually. In agreement with our results, Plotz et al. (2003) were able to express the MutL subunits hMLH1, hPMS1 and hPMS2 at high concentrations in a human MutLα deficient cell line.

It was previously reported that proteins having about 5% of RIL codons were distributed both in soluble and insoluble fractions when expressed in BL21(DE3)-CodonPlus-pRIL [42]. As shown in Fig. 3b, the fusion protein was found to be present in a soluble form and insoluble aggregates and migrated with an apparent molecular mass of 107 kDa. This molecular mass roughly corresponds to the molecular mass of the construct (102.7 kDa) fused to a His-tag (2.33 kDa). Western blot analysis of the fusion protein using anti-Histag antibodies indicated the presence of an immunoreactive band with identical molecular mass (Fig. 3c).

AtPMS1 protein purification procedure took advantage of the *N*-terminal His-tag in the fusion protein. Soluble *E. coli* extracts was applied to a Ni^+ affinity chromatography. The fusion protein bound to the resin was eluted

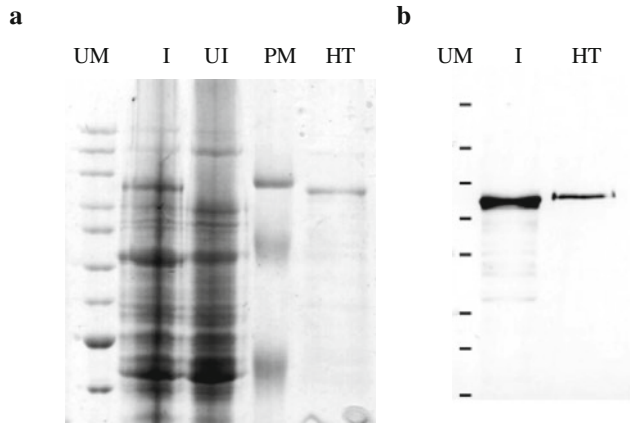

Fig. 4 **a** Purification of AtPMS1-pET28a fusion protein. Fractions were analyzed on SDS–PAGE stained with Coomassie blue. *Lane UM* unstained molecular mass markers whose values from top to bottom were 200, 150, 120, 100, 85, 70, 60, 50, 40 kDa. *Lanes I and UI* total fraction of JM109(DE3)-pRIL transformed with AtPMS1-pET28a before and after 16 hs induction with IPTG. *Lane PM* prestained molecular mass markers whose values from top to bottom were 120, 85, 50 kDa. *Lane HT* fractions from the HisTrap HP column eluted with 500 mM imidazole. The arrow indicates the position of the fusion protein. **b** Western blot analysis of AtPMS1. Primary antibodies used were the purified polyclonal antibodies generated against AtPMS1 protein. *Lane UM* unstained molecular mass markers whose values from top to bottom were 200, 150, 120, 100, 85 kDa. *Lane I* total fraction of JM109(DE3)-pRIL transformed with AtPMS1-pET28a after 16 h induction with IPTG. *Lane HT* recombinant AtPMS1-His_6 protein eluted from the HisTrap HP column

with 500 mM imidazole in the binding buffer (Fig. 4a). Analysis of the purified fractions by SDS-PAGE and Coomassie brilliant blue staining indicated a purity and yield of 99.5% and 0.2 mg/g cells, respectively.

Anti-AtPMS1 polyclonal antibodies generation

The highly purified preparation was a good candidate to immunize rabbits for polyclonal antibodies generation since *AtPMS1* gene is expressed at low levels in vivo, as described above. The immune serum was affinity purified against the denatured PMS1 protein according to Materials and Methods. Purified antibodies detected a single immunopositive protein corresponding to the fusion protein (Fig. 4b). No signal was visualized using preimmune serum (results not shown).

Conclusions

In summary, in this study we first evaluated the expression of the At*PMS1* gene in calli, flowers and seedlings and observed that this transcript is predominantly expressed in rapidly dividing tissues. This confirms the important role of the At*PMS1* gene in maintaining genomic integrity during DNA replication. We then optimized the over-expression of the *A. thaliana* PMS1 protein in *E. coli*. The presence of extra copies of the *argU*, *ileY*, and *leuW* tRNA genes, which encode tRNAs that recognize the codons AGA/AGG, AUA and CUA, respectively (pRIL) besides an extra source of $lacI^q$ repressor protein, complete *lac* deletion and *endA*, *relA* and *recA* mutations in JM109(DE3) cells, which might be responsible for tightly controlling basal expression and improving plasmid quality and stability significantly improved PMS1 expression efficiency. In addition, the protein was purified and polyclonal antibodies were generated in rabbits. The use of the recombinant protein and the antibodies will be suitable for further structure–function studies and will provide in this way a better understanding of plant DNA MMR system.

Acknowledgements We acknowledge research support from Fundación Antorchas and CONICET. RLG and CG are fellows of the Consejo Nacional de Investigaciones Científicas y Técnicas (CONICET). CPS is a member of the Researcher Career of the same institution.

References

1. Li G-M (2008) Mechanisms and functions of DNA mismatch repair. Cell Res 18:85–98
2. Kunkel T, Erie D (2005) DNA mismatch repair. Annu Rev Biochem 74:681–710
3. Iyer R, Pluciennik A, Burdett V, Modrich P (2006) DNA mismatch repair: functions and mechanisms. Chem Rev 106: 302–323
4. Jiricny J (2006) The multifaceted mismatch-repair system. Nat Rev Mol Cell Biol 7:335–346
5. Hsieh P, Yamane K (2008) DNA mismatch repair: molecular mechanism, cancer, and ageing. Mech Ageing Dev 129:391–407
6. Dzantiev L, Constantin N, Genschel J, Iyer R, Burgers P, Modrich P (2004) A defined human system that supports bidirectional mismatch-provoked excision. Mol Cell 15:31–41
7. Li G, Modrich P (1995) Restoration of mismatch repair to nuclear extracts of H6 colorectal tumor cells by a heterodimer of human MutL homologs. Proc Natl Acad Sci USA 92:1950–1954
8. Prolla T, Christie D, Liskay R (1994) Dual requirement in yeast DNA mismatch repair for MLH1 and PMS1, two homologs of the bacterial mutL gene. Mol Cell Biol 14:407–415
9. Wang T-F, Kleckner N, Hunter N (1999) Functional specificity of MutL homologs in yeast: Evidence for three Mlh1-based heterocomplexes with distinct roles during meiosis in recombination and mismatch correction. Proc Natl Acad Sci USA 96:13914–13919
10. Abdel-Rahman WM, Mecklin J-P, Peltomäki P (2006) The genetics of HNPCC: application to diagnosis and screening. Crit Rev Oncol Hematol 58:208–220
11. Bergerat A, de Massy B, Gadelle D, Varoutas PC, Nicolas A, Forterre P (1997) An atypical type II DNA topoisomerase from archaea with implication for meiotic recombination. Nature 386:414–417
12. Mushegian AR, Bassett DE Jr, Boguski MS, Bork P, Koonin EV (1997) Positionally cloned human disease genes: patterns of evolutionary conservation and functional motifs. Proc Natl Acad Sci USA 94:5831–5836

13. Dutta R, Inouye M (2000) GHKL, an emergent ATPase/kinase superfamily. Trends Biochem Sci 25:24–28
14. Hall M, Shcherbakova P, Fortune J et al (2003) DNA binding by yeast Mlh1 and Pms1: implications for DNA mismatch repair. Nucleic Acids Res 31:2025–2034
15. Ban C, Yang W (1998) Crystal structure and ATPase activity of MutL: implications for DNA repair and mutagenesis. Cell 95: 541–552
16. Guarne A, Junop MS, Yang W (2001) Structure and function of the N-terminal 40 kDa fragment of human PMS2: a monomeric GHL ATPase. EMBO J 20:5521–5531
17. Hall M, Shcherbakova P, Kunkel T (2002) Differential ATP binding and intrinsic ATP hydrolysis by amino-terminal domains of the yeast Mlh1 and Pms1 proteins. J Biol Chem 277: 3673–3679
18. Spampinato C, Modrich P (2000) The MutL ATPase is required for mismatch repair. J Biol Chem 275:9863–9869
19. Bende SM, Grafstrom RH (1991) The DNA binding properties of the MutL protein isolated from *Escherichia coli*. Nucleic Acids Res 19:1549–1555
20. Ban C, Junop M, Yang W (1999) Transformation of MutL by ATP binding and hydrolysis: a switch in DNA mismatch repair. Cell 97:85–97
21. Shcherbakova P, Hall M, Lewis M et al (2001) Inactivation of DNA mismatch repair by increased expression of yeast MLH1. Mol Cell Biol 21:940–951
22. Fukui J, Nishida M, Nakagawa T, Masui R, Kuramitsu S (2008) Bound nucleotide controls the endonuclease activity of mismatch repair enzyme MutL. J Biol Chem 283:12136–12145
23. Kadyrov FA, Dzantiev L, Constantin N, Modrich P (2006) Endonucleolytic function of MutLα in human mismatch repair. Cell 126:297–308
24. Kadyrov FA, Holmes SF, Arana ME et al (2007) Saccharomyces cerevisiae MutLα is a mismatch repair endonuclease. J Biol Chem 282:37181–37190
25. Alou AH, Jean M, Domingue O, Belzile FJ (2004) Structure and expression of AtPMS1, the *Arabidopsis* ortholog of the yeast DNA repair gene PMS1. Plant Sci 167:447–456
26. Jean M, Pelletier J, Hilpert M, Belzile F, Kunze R (1999) Isolation and characterization of AtMLH1, a MutL homologue from *Arabidopsis thaliana*. Mol Gen Genet 262:633–642
27. Jackson N, Sanchez-Moran E, Buckling E, Armstrong SJ, Jones GH, Franklin FCH (2006) Reduced meiotic crossovers and delayed prophase I progression in AtMLH3-deficient *Arabidopsis*. EMBO J 25:1315–1323
28. Murashige T, Skoog F (1962) A revised medium for rapid growth and bioassays with tobacco tissue cultures. Physiol Plant 15: 473–497
29. Sambrook J, Russel DW (2001) Molecular cloning—a laboratory manual. Cold Spring Harbor Laboratory Press, Cold Spring Harbor
30. Plaxton WC (1989) Molecular and immunological characterization of plastid and cytosolic pyruvate kinase isozymes from castor-oil-plant endosperm and leaf. Eur J Biochem 181:443–451
31. Laemmli UK (1970) Cleavage of structural proteins during the assembly of the head of bacteriophage T4. Nature 227:680–685
32. Burnette WN (1981) Western Blotting: electrophoretic transfer of proteins from sodium dodecyl sulfate-polyacrylamide gels to unmodified nitrocellulose and radiographic detection with antibody and radioiodinated protein A. Anal Biochem 112:195–203
33. Bradford MM (1976) A rapid and sensitive method for the quantitation of microgram quantities of protein utilizing the principle of protein dye binding. Anal Biochem 72:248–254
34. Spampinato CP, Gomez RL, Galles C, Lario LD (2009) From bacteria to plants: a compendium of mismatch repair assays. Mutat Res 682:110–128
35. Dion E, Li L, Jean M, Belzile F (2007) An *Arabidopsis* MLH1 mutant exhibits reproductive defects and reveals a dual role for this gene in mitotic recombination. Plant J 51:431–440
36. Li L, Dion E, Richard G, Domingue O, Jean M, Belzile FJ (2009) The *Arabidopsis* DNA mismatch repair gene PMS1 restricts somatic recombination between homeologous sequences. Plant Mol Biol 69:675–684
37. Alou A, Azaiez A, Jean M, Belzile F (2004) Involvement of the *Arabidopsis thaliana* AtPMS1 gene in somatic repeat instability. Plant Mol Biol 56:339–349
38. Li L, Jean M, Belzile F (2006) The impact of sequence divergence and DNA mismatch repair on homeologous recombination in *Arabidopsis*. Plant J 45:908–916
39. Gustafson C, Govindarajan S, Minshull J (2004) Codon bias and heterologous protein expression. Trends Biotechnol 22:346–353
40. Räschle M, Marra G, Nyström-Lahti M, Schär P, Jiricny J (1999) Identification of hMutL, a heterodimer of hMLH1 and hPMS1. J Biol Chem 274:32368–32375
41. Cutalo JM, Darden TA, Kunkel TA, Tomer KB (2006) Mapping the dimer interface in the C-terminal domains of the yeast MLH1–PMS1 heterodimer. Biochemistry 45:15458–15467
42. Rosano GL, Ceccarelli EA (2009) Rare codon content affects the solubility of recombinant proteins in a codon bias-adjusted *Escherichia coli* strain. Microb Cell Fact 8:41